Symbol error rate performance analysis of soft-decision decoded MPPM free space optical system over exponentiated Weibull fading channels

Duan Zhou (周 端)[1], Tian Cao (曹 天)[2,3,*], Yintang Yang (杨银堂)[4], Jianxian Zhang (张剑贤)[1], Ping Wang (王 平)[2,5], and Bensheng Yang (杨本圣)[2]

[1]*School of Computer Science and Technology, Xidian University, Xi'an 710071, China*
[2]*State Key Laboratory of Integrated Service Networks, School of Telecommunications Engineering, Xidian University, Xi'an 710071, China*
[3]*Southwest China Research Institute of Electronic Equipment, Chengdu 610036, China*
[4]*Key Laboratory of the Ministry of Education for Wide Band-Gap Semiconductor Materials and Devices, School of Microelectronics, Xidian University, Xi'an 710071, China*
[5]*School of Physics and Optoelectronic Engineering, Xidian University, Xi'an 710071, China*
**Corresponding author: tcao2014@163.com*

Received December 2, 2016; accepted February 17, 2017; posted online March 13, 2017

The symbol error rate (SER) performance of a multipulse pulse-position modulation (MPPM) free space optical (FSO) system under the combined effect of turbulence-induced fading modeled by exponentiated Weibull (EW) distribution and pointing errors with a soft-decision detector is investigated systematically. Particularly, the theoretical conditional SER (CSER) of soft-decision decoded MPPM is derived. The corresponding closed-form CSER is obtained via curve fitting with the Levenberg–Marquardt method. The analytical SER expression over the aggregated fading channels is then achieved in terms of Laguerre integration. Monte Carlo simulation results are also offered to corroborate the validity of the proposed SER model.

OCIS codes: 060.2605, 010.1300, 010.1330.
doi: 10.3788/COL201715.050602.

In recent years, free space optical (FSO) communication draws an enormous amount of attention because of its large capacity, low cost, secure transmission, and license-free spectrum[1,2]. It is regarded as an alternative approach to the radio-frequency (RF) technology and widely accepted to solve the "last mile" problem where fiber optic links are not practical[2,3]. However, FSO links suffer a lot from atmospheric turbulence-induced fading caused by random refractive-index fluctuations, which will result in the system performance degradation[4,5].

In order to predict the reliability of FSO channels under different strengths of turbulence, some mathematical models describing the probability density function (PDF) of the received optical scintillation have been proposed over the years, such as lognormal (LN), gamma-gamma (G-G), and exponentiated Weibull (EW) distributions. Among them, EW distribution is a novel one, which is proposed and experimentally verified by Barrios and Dios in Refs. [6,7]. Their study revealed that this distribution could model the PDF of irradiance in weak-to-strong turbulence regimes under all aperture-averaging conditions. Most importantly, apart from the perfect fit to right tail of the PDF, the left tail of EW distribution is much better than G-G and LN distributions, which is essential in assessing the outage and error performances[7]. Due to this advantage, some works concerning the performance of an FSO communication system over EW fading channels have been reported in these years[8–12].

Currently, intensity modulation with direct detection (IM/DD) is a feasible transmission scheme and popularly used in practical FSO systems, where the transmitters and receivers only modulate and detect the intensity of the carrier without its phase[13]. Among the realizations of IM/DD, on-off keying (OOK), pulse-position modulation (PPM), and multipulse PPM (MPPM) are three representative schemes. As is known, OOK is a binary level modulation type and has been extensively used in many existing works because of its simplicity and easy implementation[14]. However, OOK has lower energy efficiency so as to satisfy the requirement of the dynamic threshold at the receiver[2,15]. In order to overcome this drawback, PPM has been proposed, which is an orthogonal modulation scheme that provides a reduction in average power consumption compared to OOK, but at the expense of an increased bandwidth requirement[13,16]. This is due to the fact that the time slot when an optical pulse takes place is narrowed to increase the amount of information transmitted per signal block[17]. Although it is certainly true that a large bandwidth is easy to achieve in the optical band, spectral efficiency, from a practical perspective, is also a crucial design consideration because it is directly related to the required speed of electronic circuitry in FSO systems[2]. MPPM, proposed by Sugiyama and Nosu in Ref. [17], can substantially improve the band-utilization efficiency of optical PPM, and it could be a tradeoff between OOK and PPM. Therefore, it is

necessary to quantify the performances of MPPM-based FSO systems. So far, some works have been reported on the average bit error rate (ABER) or symbol error rate (SER) performances of the FSO system with the MPPM scheme[12,14,15,18–20]. However, only Ref. [12] is performed over EW distribution. In that work, the SER performances of the MPPM-based FSO system have been investigated with three different hard-decision thresholds: fixed decision threshold (FDT), optimized decision threshold (ODT), and dynamic decision threshold (DDT). It is demonstrated that the performance of DDT is better than those of both FDT and ODT. However, the threshold of DDT is decided with the assistance of channel state information (CSI), which will increase the complexity of the FSO system design. Besides, the impact of misalignment between the transmitter and receiver (also called pointing errors) is not considered, which is usually caused by building sway from wind loads, thermal expansion, and weak earthquakes, resulting in intensity variations of the laser beam over the receiving aperture and system performance degradation[5].

Motivated by the above analysis, the SER performance of a soft-decision decoded MPPM FSO system over composite EW fading channels with pointing errors is investigated in this work without the help of CSI. The SER performance is demonstrated systematically under different turbulence conditions with the aperture-averaging effect considered. What is more, the SER performance is compared with that of a hard-decoder-based MPPM FSO system. Monte Carlo (MC) simulation results are also offered to confirm the correctness of the theoretical results.

In this work, an IM/DD technique on the basis of MPPM is considered. The investigated FSO system has been depicted in Fig. 1. The data are directly modulated onto the intensity of an optical beam at the transmitter, which points toward a DD receiver. The laser beam propagates along a horizontal path suffering from the turbulence-induced fading. In order to mitigate such fading on the optical power, the effect of placing a collecting aperture, e.g., a lens, at the receiver end of the FSO link is employed. This phenomenon is known as aperture averaging. In this case, the received signal y at the detector can be expressed as $y = Rhx + n$, where R is the photodetector responsivity. $h = h_a h_p h_l$ represents the aggregated channel gain, where h_a is the turbulence-induced fading modeled by the EW distribution, h_p is the pointing errors loss factor, and h_l is the path loss, which is a constant at a given weather condition and link distance. Without the loss of generality, h_l is assumed to be unity throughout this work. For the (N, M) MPPM scheme of this study, the laser is pulsed in M slots in one block consisting of N slots. Assuming P_t denotes the average transmitted power, variable x is equal to NP_t/M for the signal time slot and zero for the nonsignal time slot. The noise is induced by the ambient light, which is much stronger than the desired signal at the detector, and it is assumed to include any front-end thermal noise and shot noise at the receiver[21]. Thus, n can be accurately modeled as signal-independent additive white Gaussian noise (AWGN) with zero mean and variance $\sigma_n^2 = N_0/2$. The PDF of n can be written as[4, Eq. (11.7)]

Fig. 1. Block diagram of an FSO system through the turbulent atmosphere.

$$f_n(x) = (1/\sqrt{2\pi}\sigma_n)\exp(-x^2/2\sigma_n^2). \tag{1}$$

As mentioned earlier, the EW distribution is adopted to characterize the atmospheric fading. The corresponding PDF and cumulative distribution function (CDF) of h_a can be expressed as[6]

$$f_{h_a}(h) = \frac{\alpha\beta h^{\beta-1}}{\eta^\beta}\exp\left[-\left(\frac{h}{\eta}\right)^\beta\right]\left\{1-\exp\left[-\left(\frac{h}{\eta}\right)^\beta\right]\right\}^{\alpha-1}, \tag{2}$$

$$F_{h_a}(h) = \{1-\exp[-(h/\eta)^\beta]\}^\alpha, \tag{3}$$

where $\alpha > 0$ and $\beta > 0$ are the shape parameters related to the scintillation index (SI), and $\eta > 0$ is a scale parameter related to the mean value of the irradiance. According to Refs. [6, Eqs. (10)–(12)] and [7, Eqs. (20)–(22)], it is easy to calculate those parameters. The PDF of h_p is given in Ref. [5, Eq. (11)], and the PDF and CDF of the aggregated channel gain h can be written as[8]

$$f_h(h) = \frac{\alpha\gamma^2}{\eta A_0}\left(\frac{h}{\eta A_0}\right)^{\gamma^2-1}\sum_{j=0}^{\infty} T_2(j)\Gamma[1-T_1, T_3(j)], \tag{4}$$

$$F_h(h) = \frac{\alpha\gamma^2}{\beta}\left(\frac{h}{\eta A_0}\right)^{\gamma^2}\sum_{j=0}^{\infty} T_2(j)\, G_{2,3}^{2,1}\left[T_3(j)\middle|\begin{matrix}1-T_1, 1\\ 0, 1-T_1, -T_1\end{matrix}\right], \tag{5}$$

respectively, where $\Gamma(a, z)$ is the upper incomplete gamma function. $T_1 = \gamma^2/\beta$, $T_2(j) = [(-1)^j\Gamma(\alpha)]/[j!\Gamma(\alpha-j)(1+j)^{1-T_1}]$, and $T_3(j) = (1+j)[h/(\eta A_0)]^\beta$. $A_0 = [\mathrm{erf}(\upsilon)]^2$ is the fraction of the collected optical power when the difference between the optical spot center and the detector center is equal to zero. $\upsilon = (\sqrt{\pi}a)/(\sqrt{2}\omega_Z)$ is the ratio between the aperture radius (a) and beamwidth (ω_Z) at the distance of Z, and $\mathrm{erf}(\cdot)$ is the error function. $\gamma = \omega_{Z_{eq}}/2\sigma_s$ is the ratio between the equivalent beam radius and jitter standard deviation, where $\omega_{Zeq}^2 = \omega_Z^2\sqrt{\pi}\mathrm{erf}(\upsilon)/[2\upsilon\exp(-\upsilon^2)]$.

For the (N, M) MPPM scheme, the transmission time is divided into equal successive blocks. Each block, i.e., a signal block, is further divided into N equal time slots. At the transmitter, M optical pulses are transmitted in multiple slots in a signal block. At the receiver, the received signal is detected slot by slot. Thus, the output of the sampler can be expressed as follows:

$$y_{\text{out}} = \begin{cases} \xi h + n, & \text{signal time slot}, \\ n, & \text{non-signal time slot}, \end{cases} \tag{6}$$

where $\xi = RNP_t/M$. In FSO systems, channel variations are typically much slower than the signaling period. This is because the channel coherence time is on the order of milliseconds (ms), and the data rate is assumed to be on the order of gigabits per second (Gbps)[22]. Therefore, a slow fading channel is assumed, and the instantaneous electrical signal-to-noise ratio (SNR) can be written as

$$\mu = \xi^2 h^2 / N_0 = \bar{\mu} h^2, \tag{7}$$

where $\bar{\mu}$ denotes the average electrical SNR.

It should be noted that, if there is no channel fading and noise, the signal slots should be the largest ones in the received (N, M) MPPM block. Thus, for the soft-decision decoding technique, the decoder will select the largest M slots from a received signal block (N slots), and then make those M slots be the signal time slots transmitted at the transmitter. In other words, if the transmitted symbol can be decoded correctly, the minimum value of the signal slots should be larger than the maximum value of non-signal slots in the received MPPM block. Consequently, the threshold and CSI are not required any more, therefore reducing the complexity of the practical FSO system.

In order to obtain the expression of the SER of soft-decision decoded MPPM over aggregated fading channels, the conditional SER (CSER) in absence of turbulence and pointing errors should be achieved at first. Let random variable X denote the largest value of non-signal slots, that is $X = \max(x_1, x_2, ..., x_{N-M})$, where x_i ($i = 1, 2, ..., N - M$) is the value of the ith nonsignal slot in the received signal block. Since the non-signal slots are modeled by Gaussian distribution with zero mean and variance $\sigma_n^2 = N_0/2$, the PDF of x_i can be given as

$$f_{x_i}(x) = f_n(x) = (1/\sqrt{2\pi}\sigma_n)\exp(-x^2/2\sigma_n^2). \tag{8}$$

Therefore, the CDF of x_i can be obtained as

$$F_{x_i}(x) = \int_{-\infty}^{x} f_{x_i}(x)\mathrm{d}t = Q(-x/\sigma_n), \tag{9}$$

where $Q(\cdot)$ is the Q-function. With the assistance of Ref. [23, Eq. (6–55)], the CDF of X can be achieved as

$$F_X(x) = [F_{x_i}(x)]^{N-M} = [Q(-x/\sigma_n)]^{N-M}. \tag{10}$$

By differentiating Eq. (10) with respect to (w.r.t.) x, the PDF of X can be written as

$$f_X(x) = \frac{N-M}{\sqrt{2\pi}\sigma_n}\exp\left(-\frac{x^2}{2\sigma_n^2}\right)\left[Q\left(-\frac{x}{\sigma_n}\right)\right]^{N-M-1}. \tag{11}$$

Let random variable Y represent the smallest value of the signal slots. Therefore, $Y = \min(y_1, y_2, ..., y_M)$, where y_j ($j = 1, 2, ..., M$) is the value of the jth signal slot in the received signal block. It should be noted that channel fading should not be involved during the calculation of the CSER. Therefore, y_j equals $\xi + n$. The PDF of y_j can be obtained as

$$f_{y_j}(y) = (1/\sqrt{2\pi}\sigma_n)\exp[-(y-\xi)^2/2\sigma_n^2]. \tag{12}$$

Furthermore, the CDF of y_j can be expressed as

$$F_{y_j}(y) = \mathrm{Q}[(\xi - y)/\sigma_n]. \tag{13}$$

On the basis of Ref. [23, Eqs. (6–57) and (6–58)], the CDF of Y can be obtained as

$$F_Y(y) = 1 - \{Q[(y-\xi)/\sigma_n]\}^M. \tag{14}$$

Then, the PDF of Y can be achieved by differentiating Eq. (14) w.r.t. y as follows:

$$f_Y(y) = \frac{1}{\sqrt{2\pi}\sigma_n}\exp\left(-\frac{(y-\xi)^2}{2\sigma_n^2}\right)M\left[Q\left(\frac{y-\xi}{\sigma_n}\right)\right]^{M-1}. \tag{15}$$

According to the above analysis, when the minimum value of the signal slots is greater than the maximum value of the non-signal slots, that is $Y > X$, the symbol can be decoded correctly. Let $\Psi = Y - X$, which could be rewritten as $\Psi = Y + (-X)$. The PDF of random variable $-X$ can be derived based on Eq. (11) and Ref. [23, Eq. (5–6)] as follows:

$$f_{-X}(x) = \frac{N-M}{\sqrt{2\pi}\sigma_n}\exp\left(-\frac{x^2}{2\sigma_n^2}\right)\left[Q\left(\frac{x}{\sigma_n}\right)\right]^{N-M-1}, \tag{16}$$

then, the PDF of Ψ can be expressed as the convolution of functions $f_Y(y)$ [i.e., Eq. (15)] and $f_{-X}(x)$ [i.e., Eq. (16)]

$$\begin{aligned} f_\Psi(\psi) &= f_Y(\psi) * f_{-X}(\psi) \\ &= \frac{(N-M)M}{2\pi\sigma_n^2}\int_{-\infty}^{+\infty}\left[Q\left(\frac{\varphi-\xi}{\sigma_n}\right)\right]^{M-1} \\ &\quad\times\left[Q\left(\frac{\psi-\varphi}{\sigma_n}\right)\right]^{N-M-1}\exp\left(-\frac{(\varphi-\xi)^2}{2\sigma_n^2}-\frac{(\psi-\varphi)^2}{2\sigma_n^2}\right)\mathrm{d}\varphi, \end{aligned} \tag{17}$$

Thus, the CSER expression of soft-decision decoded MPPM can be gotten via the integral of $f_\Psi(\psi)$ from negative infinity to zero (i.e., $Y < X$) as

$$P_{\mathrm{CSER}}(\sigma_n) = \int_{-\infty}^{0} f_{\Psi}(\psi)\mathrm{d}\psi. \tag{18}$$

To obtain the tractable closed-form CSER expression, the exponential fitting technique has been implemented based on the results obtained from Eq. (18). With the help of Eq. (7), the CSER w.r.t. the SNR can be written as

$$P_{\mathrm{CSER}}(\mu) = b_1 \exp(b_2\mu), \tag{19}$$

where b_1 and b_2 are exponential fitting parameters that could be obtained via the Levenberg–Marquardt method[24]. According to Eq. (7), the PDF and CDF w.r.t. μ [$f_{\mu}(\mu)$ and $F_{\mu}(\mu)$] can be obtained through Eqs. (4) and (5). Therefore, the SER expression of the soft-decision decoded MPPM FSO system over the aggregated fading channels can be expressed as

$$\begin{aligned} P_e &= \int_0^{\infty} \mathrm{CBER}(\mu) f_{\mu}(\mu)\mathrm{d}\mu = \int_0^{\infty} \mathrm{CBER}(\mu)\mathrm{d}F_{\mu}(\mu) \\ &= -\int_0^{\infty} F_{\mu}(\mu)\mathrm{dCBER}(\mu) \\ &= -b_1 b_2 \int_0^{\infty} \exp(b_2\mu) F_{\mu}(\mu)\mathrm{d}\mu. \end{aligned} \tag{20}$$

The Laguerre integration in Ref. [25] can be used to efficiently and accurately approximate Eq. (20). Finally, Eq. (20) can be rewritten as

$$P_e = -b_1 b_2 \sum_{k=1}^{m} \delta_k \exp[(1+b_2)\varepsilon_k] F_{\mu}(\varepsilon_k), \tag{21}$$

where ε_k is the kth zero of Laguerre polynomials $L_m(x)$, and the weight δ_k can be calculated by

$$\delta_k = (m!)^2 \varepsilon_k / \{(m+1)^2 [L_{m+1}(\varepsilon_k)]^2\}. \tag{22}$$

In this work, the (5, 2) MPPM is adopted to demonstrate the SER performances of the above-mentioned soft-decision decoding scheme, and the corresponding exponential fitting parameters b_1 and b_2 are 0.836 and −0.5231, respectively. The analytical SER results are obtained from Eq. (21), and m is chosen to be 15 in computing the Laguerre integration. In the process of MC simulation, a total of 1×10^8 blocks were run to reduce the statistical uncertainties of the SER. It is assumed that the receiver achieves perfect synchronization.

The SER values of (5, 2) MPPM under aggregated fading channels have been shown in Fig. 2. The EW parameters are extracted from Ref. [8]. The photodetector responsivity (R) is set to be 0.5. The link distance Z equals 1 km. The Beam half-angle divergence θ is equal to 1 mrad. Thus, the corresponding beam radius can be obtained as $\omega_Z = \theta \times Z = 1$ m. The jitter standard deviation σ_s is set to be 30 cm. The turbulence-only results (i.e., $\gamma \to \infty$) have also been presented here for comparison. As is seen, the analytical SER curves match well with the MC

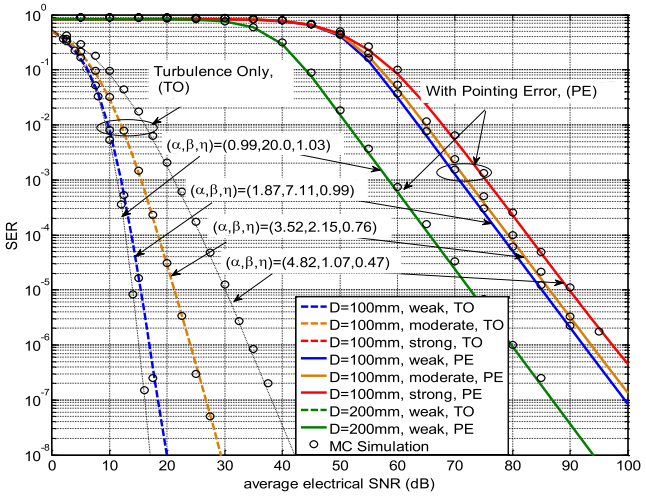

Fig. 2. Analytical SER and MC simulation results for (5, 2) MPPM under weak (Rytov variances $\sigma_R^2 = 0.32$), moderate ($\sigma_R^2 = 2.22$), and strong ($\sigma_R^2 = 15.97$) turbulence conditions. Aperture sizes are $D = 100$ and 200 mm.

simulation results over both combined fading and turbulence-only channels, verifying the correctness of our SER model. It is clearly observed that pointing errors would severely degrade the SER performance of a soft-decision decoded MPPM FSO system in the same turbulence regime and with the same aperture size. For instance, with the aperture size $D = 100$ mm, to reach the SER of 1×10^{-5}, the required electrical average SNR is about 15 dB for the turbulence-only condition, while it is 85 dB for the aggregated fading condition in the weak turbulence regime. This is because the effect of misalignment between the transmitter and receiver will decrease the power collected at the receiving aperture. However, the aperture averaging effect can mitigate this problem and improve the SER performance of a soft-decision decoded MPPM FSO system. For example, with the effect of pointing errors taken into account, to reach the SER of 1×10^{-5}, the aperture size $D =$ 200 mm offers a performance gain of about 11 dB compared with the aperture size $D = 100$ mm in terms of the average electrical SNR under the weak turbulence condition. This is because a larger aperture size can gather more transmitting power and average the intensity variations of the laser beam over the receiving aperture caused by pointing errors, thus enhancing the system performance.

Figure 3 shows the SER comparison between soft-decision decoding and the DDT[12] of hard-decision decoding schemes under moderate turbulence condition (Rytov variances $\sigma_R^2 = 1.35$) with three different aperture sizes ($D = 3$, 25, and 60 mm). The EW parameters are obtained from Ref. [6]. The analytical results of a soft-decision decoding MPPM are aquired from Eq. (21). The photodetector responsivity (R) is set to be unity. As is seen, the soft-decision decoding technique performs better than the DDT with all aperture sizes. Specifically, to reach the

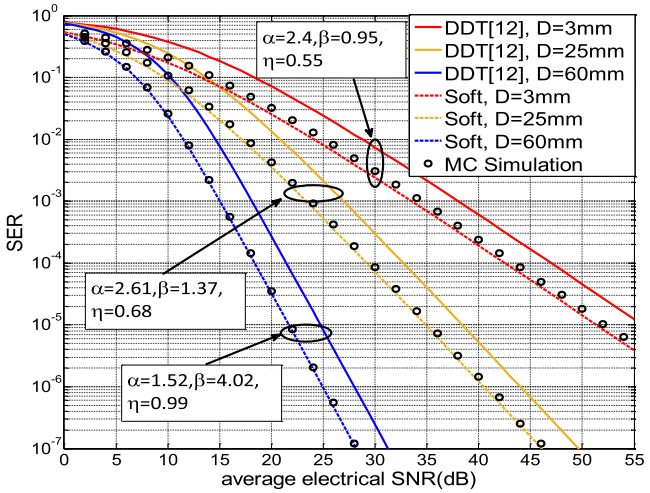

Fig. 3. SER for (5, 2) MPPM under moderate turbulence conditions ($\sigma_R^2 = 1.35$) with the soft-decision decoding technique and DDT[12] over three different receiver apertures.

same SER for all three aperture sizes, the soft decoder offers a performance gain of approximately 3.5 dB compared with the hard decoder in terms of the required average electrical SNR. Furthermore, it can be seen that the effect of aperture averaging on the SER performance of soft-decision decoding is nearly the same to that of the DDT. For instance, to achieve the SER of 1×10^{-4}, the aperture-averaged receiver (i.e., $D = 25$ mm) offers a performance gain of about 14 dB compared with the point receiver (i.e., $D = 3$ mm) in terms of the average electrical SNR for both soft-decision decoding and the DDT of hard-decision decoding schemes.

In conclusion, the closed-form SER expression of (N, M) MPPM FSO with a soft decoder over composite EW fading channels with pointing errors considered is achieved in this work. The analytical results are verified by MC simulation results. The studies show that pointing errors severely deteriorate the soft-decision decoded MPPM FSO system performance, while the aperture-average technique can mitigate this problem. Furthermore, the soft-decision decoding technique has better performance compared to the DDT, which is the best decoding method in Ref. [12]. The effect of aperture averaging on the SER performance of soft-decision decoding is similar to that of the DDT. This work is of good help for designing the MPPM FSO system with a soft decoder.

This work was supported by the National Natural Science Foundation of China (No. 61474090), the Fundamental Research Funds for the Central Universities (No. JB160105), and the 111 Project of China (No. B08038).

References

1. T. Cao, P. Wang, L. Guo, B. Yang, J. Li, and Y. Yang, Chin. Opt. Lett. **13**, 080101 (2015).
2. M. A. Khalighi and M. Uysal, IEEE Commun. Surveys Tuts. **16**, 2231 (2014).
3. T. Mao, Q. Chen, W. He, Y. Zou, H. Dai, and G. Gu, Chin. Opt. Lett. **14**, 110607 (2016).
4. L. C. Andrews and R. L. Phillips, *Laser Beam Propagation Through Random Media*, 2nd ed. (SPIE, 2005).
5. A. Farid and S. Hranilovic, J. Lightwave Technol. **25**, 1702 (2007).
6. R. Barrios and F. Dios, Opt. Express **20**, 13055 (2012).
7. R. Barrios and F. Dios, Opt. Laser Technol. **45**, 13 (2013).
8. P. Wang, X. Liu, T. Cao, H. Fu, R. Wang, and L. Guo, Appl. Opt. **55**, 7593 (2016).
9. R. Barrios and F. Dios, Proc. SPIE **8540**, 85400D (2012).
10. X. Yi and M. Yao, Opt. Express **23**, 2904 (2015).
11. S. Jiang, G. Yang, Y. Wei, M. Bi, Y. Lu, X. Zhou, M. Hu, and Q. Li, IEEE Photon. Technol. Lett. **27**, 2250 (2015).
12. P. Wang, B. Yang, L. Guo, and T. Shang, Opt. Commun. **354**, 1 (2015).
13. J. M. Kahn and J. R. Barry, Proc. IEEE **85**, 265 (1997).
14. F. Xu, M.-A. Khalighi, and S. Bourennane, J. Opt. Commun. Netw. **1**, 404 (2009).
15. T. T. Nguyen and L. Lampe, IEEE Trans. Commun. **58**, 1036 (2010).
16. P. Wang, J. Qin, L. Guo, and Y. Yang, IEEE Photon. Technol. Lett. **28**, 252 (2016).
17. H. Sugiyama and K. Nosu, J. Lightwave Technol. **7**, 465 (1989).
18. A. E. Morra, H. S. Khallaf, H. M. H. Shalaby, and Z. Kawasaki, J. Lightwave Technol. **31**, 3142 (2013).
19. J. M. Garrido-Balsells, F. J. López-González, A. Jurado-Navas, M. Castillo-Vázquez, and A. Puerta-Notario, Opt. Lett. **40**, 2937 (2015).
20. H. S. Khallaf, J. M. Garrido-Balsells, H. M. H. Shalaby, and S. Sampei, Opt. Commun. **356**, 530 (2015).
21. A. García-Zambrana, R. Boluda-Ruiz, C. Castillo-Vázquez, and B. Castillo-Vázquez, Opt. Express **22**, 23861 (2014).
22. F. Yang, J. Cheng, and T. A. Tsiftsis, IEEE Trans. Commun. **62**, 713 (2014).
23. A. Papoulis, *Probability, Random Variables, and Stochastic Processes* (McGraw–Hill, 1991).
24. W. H. Press, S. A. Teukolsky, W. T. Vetterling, and B. P. Flannery, *Numerical Recipes in C: The Art of Scientific Computing* (Cambridge University, 1992).
25. M. Abramowitz and I. Stegun, *Handbook of Mathematical Functions with Formulas, Graphs, and Mathematical Tables* (U.S. Gov. Printing Office, 1964).